frontiers | Frontiers in Energy Research

ORIGINAL RESEARCH
published: 10 May 2022
doi: 10.3389/fenrg.2022.905710

# Study on Lithium-Ion Battery Degradation Caused by Side Reactions in Fast-Charging Process

*Zhenhai Gao[1], Haicheng Xie[1], Hanqing Yu[2], Bin Ma[2], Xinhua Liu[2] and Siyan Chen[1]**

[1]College of Automotive Engineering, Jilin University, Changchun, China, [2]School of Transportation Science and Engineering, Beihang University, Beijing, China

With the development of electric vehicles, fast-charging is greatly demanded for commercialisation on lithium-ion batteries. The rapid charging process could lead to serious side reactions on the graphite anodes, such as lithium plating and solid electrolyte interface (SEI) film growth, which severely affect the battery performances. However, there is a lack of quantitative research on their contribution ratio to battery performance and the occurrence thresholds. In this work, a P2D model of a lithium-ion battery with the correction of SEI film growth and lithium plating was built. A cyclic charge/discharge experiment was also designed to analyze the changes of SEI film and lithium plating under high charge-rate conditions. It was found that under such conditions, the battery capacity attenuation in the early stage was mainly caused by lithium plating. In the middle and late stages, as the lithium plating tended to be stable, the capacity attenuation was largely caused by the growth of the SEI film. The study provides theoretical support for the improvement of the charge/discharge strategy of lithium-ion batteries.

**Keywords: lithium-ion battery (LIB), fast charging, solid electrolyte interface (SEI), lithium plating, P2D model**

OPEN ACCESS

***Edited by:***
*Shen Li,*
*Imperial College London,*
*United Kingdom*

***Reviewed by:***
*Haijun Ruan,*
*Imperial College London,*
*United Kingdom*
*Jiangong Zhu,*
*Tongji University, China*

****Correspondence:***
*Siyan Chen*
*chensiyan1987@jlu.edu.cn*

***Specialty section:***
*This article was submitted to Electrochemical Energy Conversion and Storage, a section of the journal Frontiers in Energy Research*

***Received:*** *27 March 2022*
***Accepted:*** *14 April 2022*
***Published:*** *10 May 2022*

***Citation:***
*Gao Z, Xie H, Yu H, Ma B, Liu X and Chen S (2022) Study on Lithium-Ion Battery Degradation Caused by Side Reactions in Fast-Charging Process. Front. Energy Res. 10:905710. doi: 10.3389/fenrg.2022.905710*

## INTRODUCTION

It is recorded that electric vehicles can reduce emissions by about 10–20% and pollution caused by transportation (Onat et al., 2014; Almeida et al., 2019). With the increasing number of electric vehicles, the driving range and the charging speed are getting more and more attentions, which requires continuous improvement of the energy density and the maximum charge/discharge rate of lithium-ion batteries. To meet these requirements, the electrodes of the batteries are tended to get thicker and denser (Zhang et al., 2003a; Chen et al., 2021; Zhou et al., 2021). However, as the thickness and density of the cathodes of the batteries increase, the electrolyte is difficult to fully enter the electrode, increasing the possibility of lithium plating on the anode and the risk of safety (Doyle and Newman, 1995; Zhang et al., 2003b; Ouyang et al., 2015; Waldmann et al., 2018; Tomaszewska et al., 2019). Thermodynamically, under normal conditions, the reaction enthalpy of lithium-ion plating is greater than that of lithium-ion insertion, and it is difficult for lithium plating to occur (Legrand et al., 2014; Gao et al., 2021). However, during the charging process, an induced overpotential is formed due to the shift in equilibrium, which may cause the potential of graphite particles to drop below 0 V, resulting in the lithium plating (Hein and Latz, 2016). The lithium plating is a serious side reaction, which would severely consume the amount of cyclable lithium in the battery. It can also lead to a reduction in battery capacity and an impaired safety of the batteries (Fleischhammer et al., 2015; Yang et al., 2020; Su et al., 2021; Zhang et al., 2022).

Another cause of loss of lithium inventory (LLI) in lithium-ion batteries is the overgrowth of SEI film (Matadi et al., 2017). During the first charge/discharge cycle of a lithium-ion battery, the electrode material reacts with the electrolyte at the solid-liquid phase interface, forming a passivation layer covering the surface of the electrode. The process is called the chemical formation. The passivation layer is the SEI film, which is an interface layer with the characteristics of a solid electrolyte. It is insulated against electrons, but $Li^+$ can enter and exit freely. Although the SEI films are formed on both cathode and anode, the SEI film on the cathode has much less influence than that on the anode (Guan et al., 2018). After numerous charge/discharge cycles, the SEI film on the anode surface would gradually increase (Klett et al., 2014), which would consume lithium-ions and cause the battery capacity to gradually decay (Barré et al., 2013; Stiaszny et al., 2014). Usually, the SEI film and lithium plating would affect each other. When the battery is charged at high current rates or the ionic conductivity of the SEI film is significantly reduced at low temperatures, lithium-ions cannot be embedded in the anode in time, and they would accumulate on the SEI film, resulting in lithium plating. The plating of lithium is generally reversible, and the plated lithium would be re-oxidized at about 0.1 V, which is much lower than the potential of delithiation of the anode (Burow et al., 2016). Therefore, the plated lithium would dissolve into recyclable lithium-ions during discharge. However, the two side effects could affect each other. The lithium plating would cause the SEI film damage, forcing the regeneration and increasing of the SEI film (Koleti et al., 2020). In addition, a secondary SEI film can also be formed on the plated lithium surface (Zhao et al., 2019).Due to the uneven deposition of lithium on the surface of the anode, some protrusions will be formed on the surface of the SEI film, making the SEI film uneven (Lewerenz et al., 2017; Wu et al., 2020). With the continuous progress of lithium plating, some protrusions would grow into lithium dendrites, which would penetrate the separator, causing internal short circuits and thermal runaway of lithium batteries. It could seriously affect the safety of lithium-ion batteries (Ecker et al., 2017a). In addition, during the lithium plating process, some of the plated lithium would be fractured and exfoliated. When the plated lithium is completely covered by the SEI film, they would become "dead lithium," causing irreversible loss of cyclable lithium (Zhao et al., 2019; Zhu et al., 2020; Lin et al., 2021; Zhu et al., 2021; Choi and Park, 2022)。

It can be concluded that the lithium plating and SEI film growth have an impact on the battery performance, influencing cycle ability and safety of lithium-ion batteries. In addition to the LLI phenomenon, the relevant literature also shows that loss of active material (LAM) will also affect the battery performance, which is usually caused by materials mechanical pulverization, metal dissolution, graphite exfoliation and electrolyte decomposition, resulting in the decline of battery capacity (Xie et al., 2021; Ruan et al., 2022).

Different from the equivalent circuit model (ECM) that only describes the output characteristics of lithium-ion batteries, the electrochemical model is based on the laws of physics to describe the real electrochemical behavior inside the battery (Plett, 2015; Schimpe et al., 2018). Currently, electrochemical lithium-ion battery models include microscale models, pseudo three-dimensional models (P3Ds), P2D models and single particle models (SPMs). Among them, the microscale model is complex and computationally expensive, which is not suitable for battery diagnosis. Therefore, most researches on battery state diagnosis based on electrochemical models generally uses SPMs or various reduced-order models (ROMs) to improve computational efficiency (Khalik et al., 2019). These electrochemical models are computationally small and generally have efficient simulation performance; however, they could not well describe the battery behavior under high current rates charge/discharge with severe gradient distribution of internal particles (Xia et al., 2017). In this work, to balance the above two models, a P2D model was proposed, which could truly simulate the electrochemical behavior of the battery within the acceptable calculation scale (Han et al., 2021).

In practice, the control of lithium plating and SEI film growth is very important (Gao and Tang, 2008; Sturm et al., 2019; Li et al., 2021). In this research, a P2D model of $LiNi_{0.8}Co_{0.15}Al_{0.05}O_2$ ternary lithium-ion battery was built, and the correction of SEI film and lithium plating was added to simulate the internal changes of lithium-ion battery during charge/discharge. In the follow-up experiments, we designed a cyclic charge/discharge experiment, focusing on analyzing the changes of the SEI film and the lithium plating on the anode under high current rate charge/discharge conditions, as well as their contributions to the battery aging at different cycle stages.

# METHODS AND MODEL

## Li-Ion Battery P2D Model and Its Parameters

In this work, the P2D model was modified to simulate aging process of lithium-ion batteries, which was first introduced by Doyle et al. (Yang and Wang, 2018). In the following, the governing equations were briefly reviewed and the schematic diagram of the model was shown in **Figure 1** where the electrochemical behaviors of lithium-ions and electrons during discharge were described.

The model takes into account the transport of charges and species in the active material along the electrode thickness direction ($x$) and within solid particles ($r$), and $x$ and $r$ directions describe the coupling of electrochemical reactions on the surface of active material particles *via* the Butler-Volmer kinetics (Ecker et al., 2017b; Momeni Boroujeni and Birke, 2019).

$$j_{In} = a_s i_0 \left( \exp\left( \alpha \eta F / RT \right) - \exp\left( -(1-\alpha)\eta F / RT \right) \right) \quad (2.1)$$

And $i_0$ is concentration-dependent exchange current density

$$i_0 = kFc_e^{\alpha}(c_{max} - c_s)^{\alpha} c_s^{1-\alpha} \quad (2.2)$$

Where $j_{In}$ is the intercalation current density of lithium-ion, $a_s$ is the volume-specific active area, $\alpha$ the symmetry coefficient of the reaction, $\eta$ is the electrochemical overpotential, $k$ the reaction rate constant, $c_e$ is the $Li^+$ concentration in electrolyte, $c_s$ is the $Li^+$

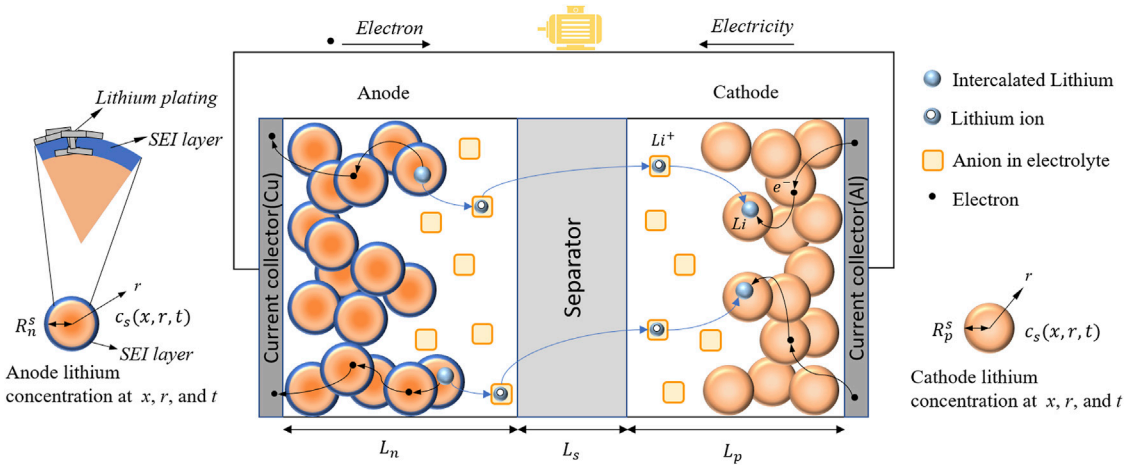


**FIGURE 1 |** Schematic diagram of the modified P2D model of lithium-ion batteries.

concentration in active material, and $c_{max}$ is the maximal $Li^+$ concentration in active material. Diffusion of lithium-ion in spherical particles is described by Fick's law in a radial coordinate r:

$$\frac{\partial c_s}{\partial t} = \frac{1}{r^2}\frac{\partial}{\partial r}\left(D_s r^2 \frac{\partial c_s}{\partial r}\right) \tag{2.3}$$

Where $D_s$ is the solid-phase diffusion coefficient. Further, initial values $c_{a0}$ and $c_{co}$ are introduced for the solid-phase volume elements of anode and cathode at $t = t_0$. Respectively, in the electrolyte, diffusion and migration are considered as following:

$$\varepsilon \frac{\partial c_e}{\partial t} = \frac{\partial}{\partial x}\left(D_{e,eff}\frac{\partial c_e}{\partial x}\right) + \left(1 - t_p\right)\frac{j_{In}(x)}{F} \tag{2.4}$$

And the liquid-phase potential $\phi_0$ could be governed as following:

$$\phi_e = -\frac{\partial}{\partial x}\left(\sigma^e_{eff}\frac{\partial c_e}{\partial x}\right) + \left(1 - t_p\right)\frac{j_{In}(x)}{F} \tag{2.5}$$

Where $\sigma^e_{eff}$ is the effective electrolyte conductivity, $x$ is a linear coordinate orthogonal to the plain electrode area, and $t_p$ is the transference number. The effective diffusion coefficient is derived from porosity $\varepsilon$ and tortuosity $\tau$ as following:

$$D^e_{eff} = D_e\frac{\varepsilon}{\tau} \tag{2.6}$$

Further, to investigate the influence of lithium plating and SEI film growth on cyclic aging of lithium-ion batteries, two correction terms were added into the P2D model (Reniers et al., 2019), where two reactions competes with intercalation reactions during charge. And the current density of the total reaction $j_{tot}$ could be redefined as following:

$$j_{tot} = j_{In} + j_{Pl} + j_{SEI} \tag{2.7}$$

Where $j_{In}$ is the intercalation current density of lithium-ions into the anode particles, $j_{SEI}$ is the current density of SEI film formation, $j_{Pl}$ current density of lithium plating.

According to the Butler-Volmer kinetics, the intercalation current density of lithium-ions entering the negative electrode particles can be obtained as following.

$$j_{In} = \frac{k_{In}\sqrt{c_e c_s^{\star}\left(c_s^{max} - c_s^{\star}\right)}}{F}\left(\exp\left(\frac{F - F\alpha}{RT}\eta_{In}\right) - \exp\left(-\frac{F\alpha}{RT}\eta_{In}\right)\right) \tag{2.8}$$

Furthermore, it is assumed that the reaction of the SEI film is irreversible (Müller et al., 2019), and there is no secondary SEI film formed on the lithium plating surface. The current density of SEI film could be defined as following:

$$j_{SEI} = -a_s\left(nFk_{SEI}c_s\right)\exp\left(\frac{nF\alpha}{RT}\eta_{SEI}\right) \tag{2.9}$$

It is assumed that there is not the dissolution of lithium and the generation of "dead lithium" in the reaction. The expression of lithium plating in the model is similar to that of SEI film growth:

$$j_{Pl} = -a_s\left(nFk_{Pl}\boldsymbol{c_s}\right)\exp\left(\frac{nF\alpha}{RT}\eta_{Pl}\right) \tag{2.10}$$

The solid phase particles and the electrolyte also meet the basic rules of mass conservation and charge conservation. The charge conservation of the solid phase particles could be defined as following:

$$\frac{\partial}{\partial x}\left(\sigma_{eff}\frac{\partial \Phi_s}{\partial x}\right) = jFa_s \tag{2.11}$$

Accordingly, the mass conservation equation of solid phase particles:

**TABLE 1 |** Symbols and descriptions of the P2D model parameters.

| Symbol | Value | Description |
|---|---|---|
| $c_s^{max}$ | 31,507 | Maximum lithium concentration in solid phase [$mol/m^3$] |
| $\sigma_{eff}$ | 100 | Effective solid particle conductivity [$S/m$] |
| $D_{eff}^s$ | $1.6 \times 10^{-14}$ | Effective solid particle diffusivity [$m^2/s$] |
| $\varepsilon_{p,n,s}$ | 41,44,37 | Porosity [%] |
| $t_+$ | 0.38 | Transference number [-] |
| $\alpha$ | 0.5 | Transfer coefficient of the reaction [-] |
| $F$ | 96,485 | Faraday's constant [$C/mol$] |
| $R$ | 8.314 | Universal gas constant [$J/(mol \cdot K)$] |
| $\phi_s$ | — | Solid particle potential [$V$] |
| $\phi_e$ | — | Electrolyte potential [$V$] |
| $c_s$ | — | Lithium concentration in solid phase [$mol/m^3$] |
| $c_e$ | — | Lithium concentration in electrolyte phase [$mol/m^3$] |
| $c_s^*$ | — | Lithium concentration at surface in solid phase [$mol/m^3$] |
| $\kappa_{eff}$ | — | Effective electrolyte conductivity [$S/m$] |
| $D_{eff}^e$ | — | Effective electrolyte diffusivity [$m^2/s$] |
| $k_{In,Pl,SEI}$ | — | Reaction rate constant of intercalating, plating and SEI [$m/s$] |
| $a_s$ | — | specific surface area [1/m] |
| $j_{In,Pl,SEI}$ | — | Ionic flux of intercalating, plating and SEI [$A/m^3$] |
| $\eta_{In,Pl,SEI}$ | — | Overpotential of intercalating, plating and SEI [$V$] |
| $T$ | — | Temperature [$K$] |

*The subscripts p, s, and n represent the anode, the separator, and the cathode, respectively.*

$$\frac{D_{eff}^s}{r^2}\frac{\partial}{\partial r}\left(r^2\frac{\partial c_s}{\partial r}\right) = \frac{\partial c_s}{\partial t} \tag{2.12}$$

The charge conservation equation of electrolyte:

$$\frac{2RT(1-t_+)}{F}\frac{\partial}{\partial x}\left(\kappa_{eff}\frac{\partial \ln c_e}{\partial x}\right) - \frac{\partial}{\partial x}\left(\kappa_{eff}\frac{\partial \Phi_e}{\partial x}\right) = jFa_s \tag{2.13}$$

And the Mass-conservation equation of electrolyte:

$$\varepsilon_s\frac{\partial c_e}{\partial t} = \frac{\partial}{\partial x}\left(D_{eff}^e\frac{\partial c_e}{\partial x}\right) \tag{2.14}$$

$$\varepsilon_{p,n}\frac{\partial c_e}{\partial t} = \frac{\partial}{\partial x}\left(D_{eff}^e\frac{\partial c_e}{\partial x}\right) + \frac{(1-t_+)}{F}j \tag{2.15}$$

All the above equations build the framework of the battery model, and all spatial derivatives are discretized by finite volume method. The description of all parameters can be found in **Table 1**.

## Simulation Design and Data Processing

The discharge cut-off voltage of the battery was set to 2.5 V. Then, it was charged with constant current at 1 C. When the voltage reached 4.1 V, it was under constant voltage charging until the charging current was less than C/20. The battery was then discharged with constant current at 1 C until the voltage reached 2.5 V. It should be noted that there was a rest for 10 min after each charge or discharge.

To reduce the computational cost, an aging factor of decay = 100 is introduced in the process of lithium plating and SEI film growth, in 2000- cycle groups. (Abdel- Monem et al., 2017),Therefore, each cycle here is equivalent to 100 cycles. Namely, only 20 cycles need to be calculated for 2000 cycles in practice. The battery information and experimental design can be found in **Table 2** and **Table 3**.

SEI film thickness, lithium plating thickness, relative discharge capacity and relative capacity of cyclable lithium are defined for results and discussions, whose calculation formulas are provided as Eqs 2–16 to Eqs 2)–(19. The related parameters are shown in **Table 4**.

$$Discharge\ capacity\ (-) = \frac{t_e - t_s}{1\,[h]} \tag{2.16}$$

$$Lithium\ inventory\ (-) = \frac{Li_i - Li_c}{Li_s} \tag{2.17}$$

$$Thickness\ lithium\ plating\ (\mathrm{nm}) = \frac{c_{Pl}M_{Pl}}{\rho_{Pl}}As_{Pl} \tag{2.18}$$

$$Thickness\ SEI\ film\ (\mathrm{nm}) = \frac{c_{SEI}M_{SEI}}{\rho_{SEI}}As_{SEI} \tag{2.19}$$

# RESULTS AND DISCUSSION

**Figures 2**, **3** show the capacity curves of the cell with respect to different temperatures and current rates under long-cycle conditions, respectively. It can be found that as the number of cycles increases, the capacity of the cell decreases continuously. It means that during gradual degradation, the available lithium-ion of the battery is continuously depleted, which directly lead to a continuous decrease of available discharge capacity. At the same time, the significant difference between the discharge capacity decay curve and the cell capacity retention curve indicates that a considerable amount of available lithium-ion is solidified in the battery during the process. In addition, the slope changes of the two curves of indicates changes in the proportion of the non-recoverable part of the solidified lithium-ion. A large slope means a considerable loss of available lithium-ion in a short term. Accordingly, it can be found that the decay rate of the battery

**TABLE 2 |** Basic parameters of battery.

| LIB chemistry | Capacity | Operational voltage range | Operational current | Maximum current (C) |
|---|---|---|---|---|
| NCA | 3.2 (Ah) | 2.5–4.1(V) | 3.2 (A) | 5 |

**TABLE 3 |** Sets of experiment groups.

| Number | Temperature and current rate |
|---|---|
| Group 1 | 3 sets of cells were charged/discharged at 0, 25, 40°C with 1 C |
| Group 2 | 3 sets of cells were charged/discharged at 25°C with 1, 2 and 3 C |
| Group 3 | 5 sets of cells were charged/discharged at 25°C with 1–5 C |
| Group 4 | 4 sets of cells were charged/discharged at 0, 10, 25, 40°C with 3 C |

**TABLE 4 |** Parameters related to evaluation indicators.

| Symbol | Description |
|---|---|
| $t_e$ | End time of discharge [*s*] |
| $t_s$ | Start time of discharge [*s*] |
| $Li_i$ | Initial lithium inventory [$C/m^2$] |
| $Li_c$ | Consumption of lithium inventory [$C/m^2$] |
| $c_{PI}$ | Molar concentration change caused by lithium plating [$mol/m^3$] |
| $c_{SEI}$ | Molar concentration change caused by SEI film [$mol/m^3$] |
| $M_{PI}$ | Molar mass of lithium plating [$kg/mol$] |
| $M_{SEI}$ | Molar mass of SEI film [$kg/mol$] |
| $\rho_{PI}$ | Density of lithium plating [$kg/m^3$] |
| $\rho_{SEI}$ | Density of SEI film [$kg/m^3$] |
| $As_{PI}$ | active specific surface area of lithium plating [1 /*m*] |
| $As_{SEI}$ | active specific surface area SEI film [1 /*m*] |

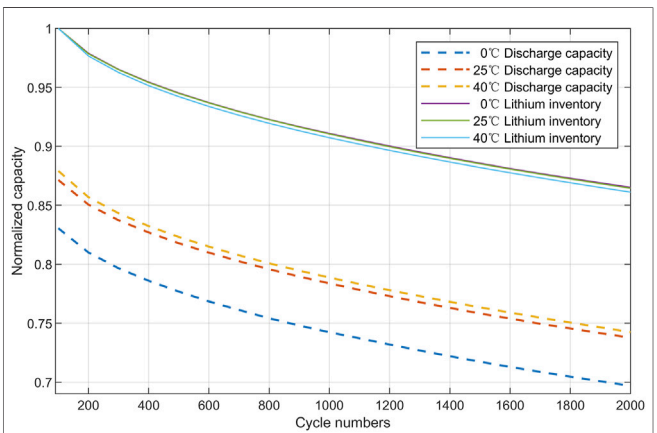


**FIGURE 2 |** Influence of temperature on charging capacity and available lithium-ion decrease.

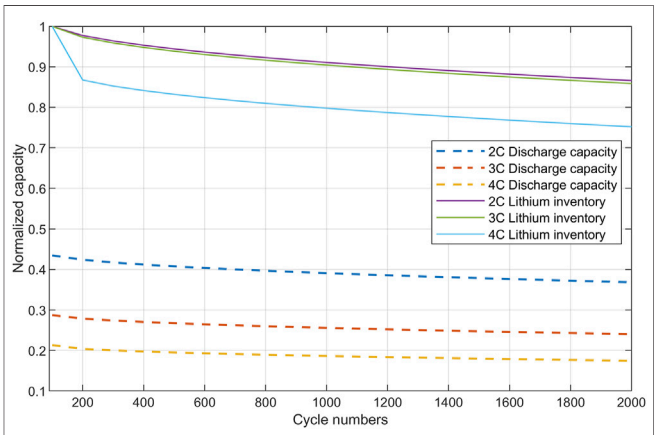


**FIGURE 3 |** Influence of charge rate on charging capacity and available lithium-ion decrease.

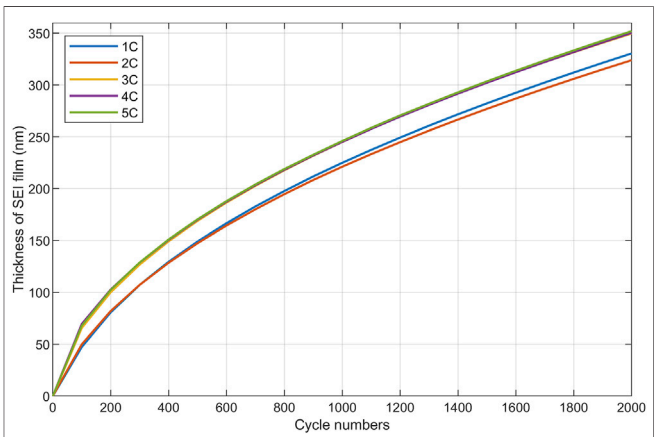


**FIGURE 4 |** Influence of charge rate on SEI film growth at room temperature.

in early cycles is significantly faster than that in late cycles, and the capacity retention rate gradually approach a constant value in late cycles. The available discharge capacity curve is sensitive to both low temperatures and high charge rates, while the capacity retention curve is more sensitive to the rate factor than the temperature factor. The retention curve of 4C capacity in **Figure 2** even shows a significant inflection point in early cycles. The reasons for these phenomena would be discussed in detail after the reason of available lithium-ion loss was analyzed.

It was reported that the loss of available lithium-ion was due to the performance degradation caused by SEI growth and lithium plating (Jaguemont et al., 2016; Jiang et al., 2016; Zhao et al., 2018; Han et al., 2021). To clarify the contributions of these decay mechanisms at different stages and their activation thresholds under different working conditions, the thickness of SEI film and lithium plating was further investigated. The results were shown in **Figures 4–6**.

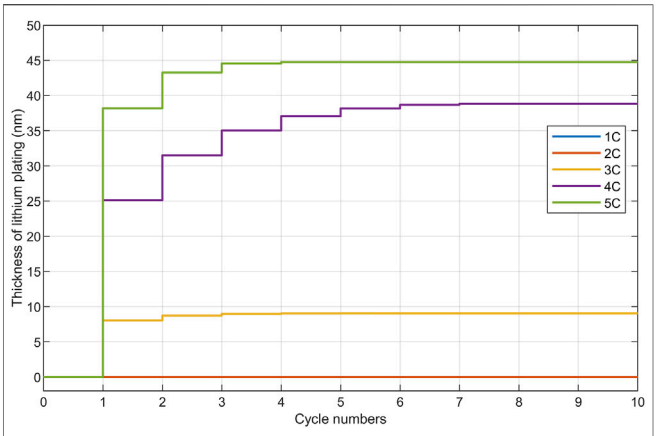


**FIGURE 5 |** Influence of charge rate on lithium plating thickness at room temperature.

**Figure 4** showed the thickness change of SEI film under long-cycle conditions. It showed that the thickness of SEI film was approximately linearly related to the number of cycles. At the same time, the variation trend of the SEI film thickness and the battery capacity decay in middle and later cycles were highly consistent. Therefore, it was speculated that the battery capacity decay in middle and late cycles was mainly caused by SEI generation, while the rapid lithium-ion loss in early cycles was caused by other decay mechanisms. Furthermore, we found that the SEI film formation was insensitive to the charging rate. In **Figure 4**, there was basically no detectable change of SEI film under the conditions of high charge rates (i.e., 3–5 C). However, under the conditions of medium charge rates (i.e., 1–2 C), the equilibrium thickness of the SEI film was slightly thinner than that under high charging rate conditions. At 2 C, the SEI film thickness at late cycles was even thinner than that at 1 C. This also proved that charge rates was not a sensitive factor for the SEI film growth.

**Figures 5**, **6** showed the growth of lithium plating with the increasing number of cycles under the same long-cycle conditions. As the process of lithium plating would quickly reach equilibrium in early cycles under all working conditions, which could also be proved by Je's group (Zhang et al., 2021).**Figures 5**, **6** only displayed early cycles of the process of lithium plating formation. Basically, the lithium plating was very obvious in early cycles, and the thickness tended to stabilize rapidly as the number of cycles increases, suggesting that the formation of lithium plating was responsible for the rapid decline of battery performance in early cycles. Furthermore, it was found that there was an obvious threshold in terms of charge rate for the lithium plating. As shown in **Figure 5**, at 25°C, under medium charge rates, the process of lithium plating could not occur; while under high charge rates, it became more and more obvious with the increase of charge rate. The equilibrium thickness of lithium plating had a monotonically positive correlation with charge rate. **Figure 6** showed that low temperature would significantly aggravate the lithium plating. These results basically explained the rapid performance degradation at early cycles. The increase of charge rate and SOC would also aggravate lithium plating, resulting in stronger degradation. Meanwhile, according to automotive standards, a capacity retention rate of 80% usually indicates end-of-life (EOL), i.e., SOH = 80%. The increase in charge rate and the decrease in temperature would actually shift the EOL to lower cycle numbers and thus shorten the lifetime of the battery (shown in **Figures 1**, **2**). The result is consistent with other researches, which reported that the cycle life was about 90–140 cycles at the low temperatures (Fan and Tan, 2006), while at higher temperature (i.e., 45°C), the cycle life was more than 2000 cycles (Abdel- Monem et al., 2017). Generally, lithium plating can lead to serious performance degradation, and at high charge rates and low temperatures, the contribution of lithium plating is significantly higher than that of SEI film growth.

Variation regularity of lithium plating thickness with different charge rates and different temperatures was shown in **Figure 7**. Under high charge rates (i.e., 3–4 C), compared with the normal temperature of 25°C, the thickness of lithium plating was significantly higher than that at low temperatures, which was consistent with existing researches. And the trend was shown in **Figure 6** (Waldmann et al., 2014; Yang et al., 2018). However, at 45°C, the thickness of lithium plating tended to increase. Therefore, lithium plating differs from other degradation processes in terms of temperature dependence. Danzer and Mehrense reported the same findings (Fan and Tan, 2006; Waldmann et al., 2014), considering it was caused by low-temperature charging, high current and high state of charge (SOC). They also found that poor capacity balance would lead to metal lithium plating at a relatively high temperature. In addition to capacity loss and impedance rise, the lithium plating can also cause an internal short circuit in the battery, resulting with a serious safety hazard (Waldmann et al., 2014; Tippmann et al., 2014). Zhang's study (Chandrasekaran, 2014) showed that during low-temperature charging, the intercalation of lithium-ion in graphite particles and the lithium plating on the particle surface competed with each other, while high charge rate currents led to limited charge transfer at the particle/SEI interface. However, some researchers (Waldmann et al., 2018)

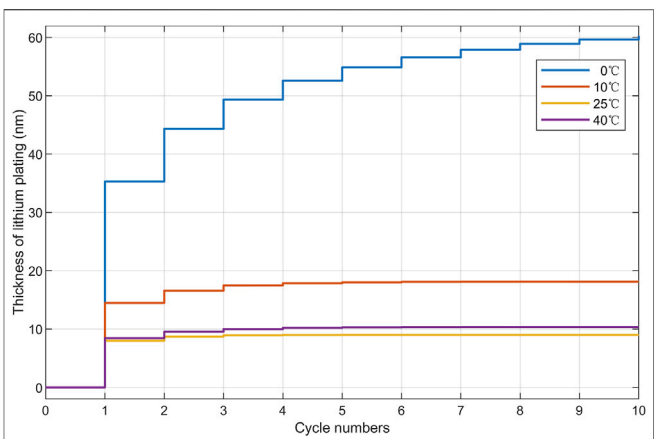


**FIGURE 6 |** Influence of temperature on lithium plating thickness charged under 3C.

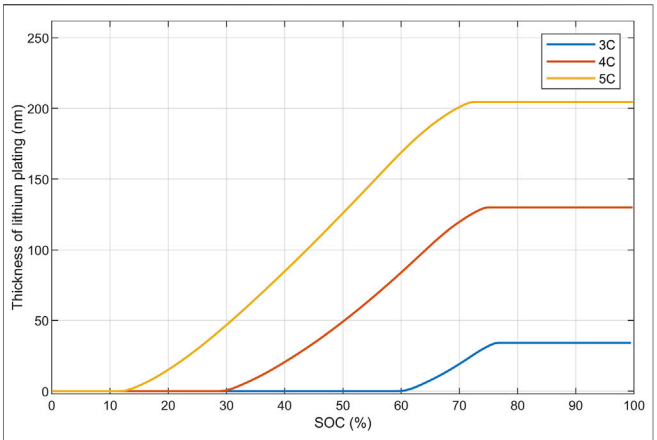


**FIGURE 7 |** Influence of charge rate on lithium plating thickness at different temperatures.

believed that low temperature would reduce the ionic conductivity of SEI film, resulting in the inability of lithium-ions to quickly enter the anode, thereby accumulating on the surface of the SEI film to form metallized deposits. This explains the reason for the sudden and sharp thickening of the lithium plating caused by the high charge rate charging at low temperatures, as shown by the 0°C curve in **Figure 6**. The rapid decrease in lithium-ion mobility and the increase of the carrier concentration in the anode region jointly limited the transport process of lithium-ion. To verify above speculation, the specific growth process of lithium plating in a single cycle was further studied in **Figure 8**. It was found that at 0°C, the lithium plating induced by high charge rates (i.e., 3–5 C) was significantly intensified as the charge rates increased. And, lithium plating only occurred at high SOC conditions. This was consistent with Danzer's findings (Fan and Tan, 2006). When the graphite potential decreased below 0 V with respect to $Li/Li^+$, lithium plating would occur. If the diffusion of lithium-ion in the graphite particles was too slow, the particle surface would be saturated with lithium-ions, resulting in lithium plating (Klett et al., 2014).

In summary, the emergence of lithium plating was essentially due to the limited large-scale transport of lithium-ion. When the lithium plating conditions were met, the lithium platting phenomenon would occur in early cycles and reach the plating-dissolution equilibrium after several cycles. Low temperature and high charge rate conditions would aggravate the lithium plating. And, high charge rate charging would lead to insufficient SEI film conduction capability, resulting in lithium-ion accumulation on the top of the SEI film.

To quantify the contributions of lithium plating and SEI film growth to the active lithium-ion loss in the battery under working conditions, we investigated the contributions of lithium platting and SEI film growth to the decayed capacity at different charge rates and temperatures (shown in **Figure 9**). For the same reason to **Figures 5**, **6**, only early cycles were displayed in the figures. It showed that although both lithium plating and SEI film growth would consume available lithium-ion, the consumption by the formation of SEI film was almost negligible under low temperature conditions, and lithium plating was almost the only decay mechanism under this condition, which is consistent with Danzer's research (Fan and Tan, 2006). And then, it was found that when the temperature and current reached the lithium plating conditions, the process of lithium plating would occur rapidly and consume a large amount of available lithium-ion. As shown in **Figure 9A**, the high charge rates at 0 °C could even led to a loss of nearly 10% of the available capacity in the short term. It could also be noticed that after certain cycles, the thickness of lithium plating would reach dynamic equilibrium without causing further loss of available lithium-ion, which was consistent with the results represented by Monroe (Zinth et al., 2014; Somerville et al., 2016). In the meanwhile, the lithium-ion loss caused by SEI film formation increased linearly with the number of cycles, which had no significant

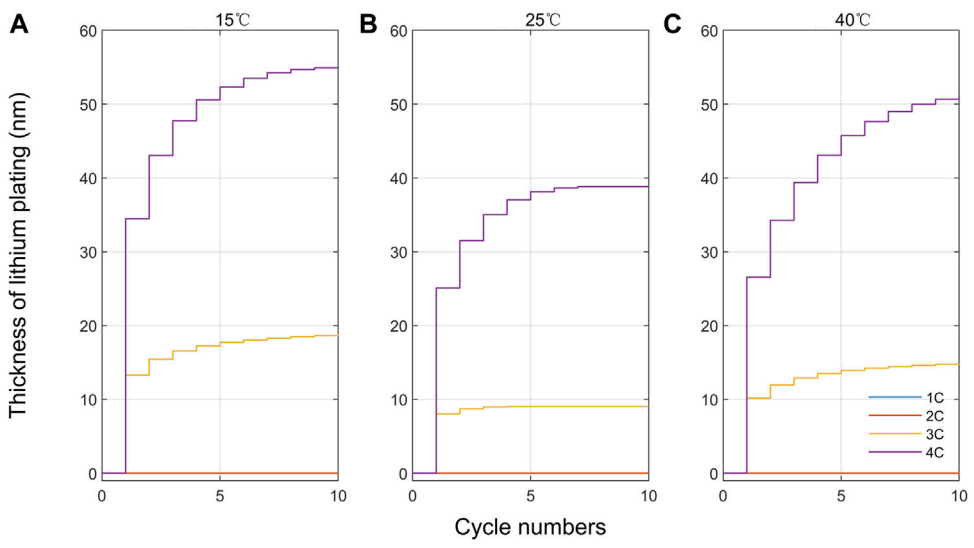


**FIGURE 8 |** Relationship of lithium plating thickness and cell SOC charged under high charge rate at 0°C.

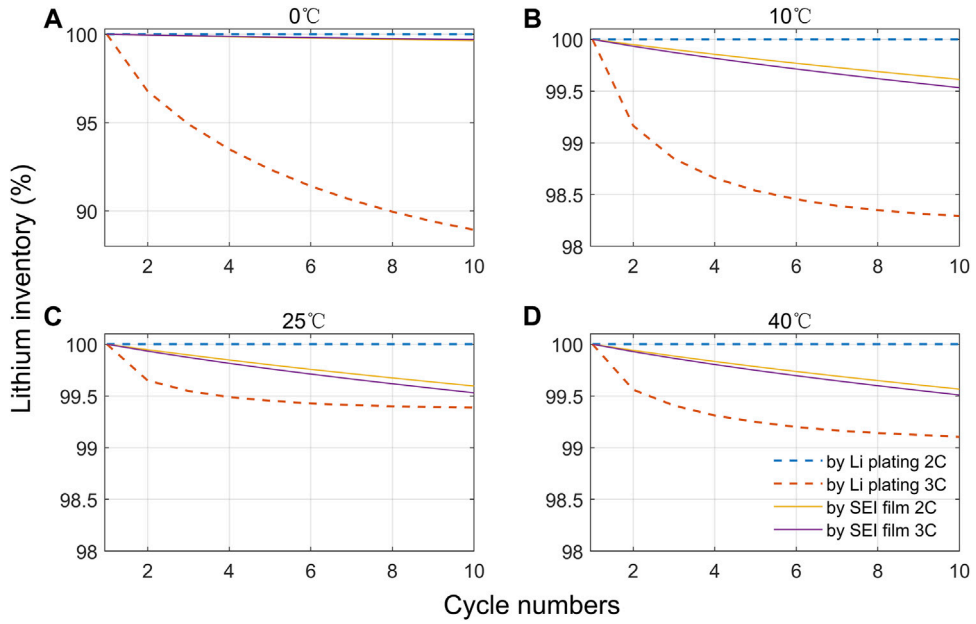


**FIGURE 9 |** Contributions of lithium plating and SEI film growth charged under different charge rates at different temperatures.

relationship with the current. And, the continuous accumulation became the dominant factor in middle and late cycles. To sum up, the unreasonable use of the battery (e.g., low temperatures and high charge rates) could lead to the formation of lithium plating at early cycles, causing serious capacity loss and significantly accelerating the aging of the battery. However, the influence of lithium plating was limited to early cycles, as it was rapidly achieved under the combined effect of the reaction potential and the diffusion rate. In middle and late cycles, the continuous available lithium consumption caused by SEI film formation and the withdrawal of the lithium plating mechanism, making it the main cause of lithium loss at this stage. As the capacity decay rate caused by which was approximately linear and was not sensitive to the charge rate, a good battery temperature control system could effectively suppress the battery aging at this stage. At the same time, since the lithium loss caused by lithium plating would reach the maximum only under both low temperature and high charge rates, well-controlled battery temperature could effectively offset the negative effect of fast charging on battery capacity.

## CONCLUSION

In this study, the corrections of SEI film and lithium plating were added to the P2D model of the battery, and a series of battery cycle aging simulation experiments were carried out using the corrected P2D model, aiming to analyze the contributions of SEI film and lithium plating on battery aging under high charge rate conditions. Through the simulation experiments, it was found that under the high charge rate conditions, the battery capacity attenuation in the early cycles were mainly caused by lithium plating; in middle and late cycles, the thickness of lithium plating tended to be stable, and the capacity attenuation at this stage was caused by the growth of SEI film. At the same time, it was also found that the lithium plating was significantly intensified at low temperature and high charge rates charging conditions. Thus, a good cell temperature control would have a significant inhibitory effect on lithium plating and SEI film, which could partially offset the negative impact of fast charging on battery capacity. This research would provide theoretical support for the improvement of charging and discharging strategies for lithium-ion batteries.

## DATA AVAILABILITY STATEMENT

The original contributions presented in the study are included in the article/Supplementary Material, further inquiries can be directed to the corresponding author.

## AUTHOR CONTRIBUTIONS

ZG:Conceptualization, Writing—Original Draft HX:Software, Visualization HY:Investigation, Validation BM:Data Curation XL:Supervision SC:Supervision Methodology, Writing—Review and Editing.

## FUNDING

This work is supported by the Science and Technology Development Project of Jilin province (20200501012GX) and National Natural Science Foundation of China (No. 52102470).

## REFERENCES


Abdel-Monem, M., Trad, K., Omar, N., Hegazy, O., Van den Bossche, P., and Van Mierlo, J. (2017). Influence Analysis of Static and Dynamic Fast-Charging Current Profiles on Ageing Performance of Commercial Lithium-Ion Batteries. *Energy* 120, 179–191. doi:10.1016/j.energy.2016.12.110

Almeida, A., Sousa, N., and Coutinho-Rodrigues, J. (2019). Quest for Sustainability: Life-Cycle Emissions Assessment of Electric Vehicles Considering Newer Li-Ion Batteries[J]. *Sustainability* 11 (8), 822–835. doi:10.3390/su11082366

Barré, A., Deguilhem, B., and Grolleau, S. (2013). A Review on Lithium-Ion Battery Ageing Mechanisms and Estimations for Automotive Applications[J]. *J. Power Sources* 241, 680. doi:10.1016/j.jpowsour.2013.05.040

Burow, D., Sergeeva, K., Calles, S., Schorb, K., Börger, A., Roth, C., et al. (2016). Inhomogeneous Degradation of Graphite Anodes in Automotive Lithium Ion Batteries under Low-Temperature Pulse Cycling Conditions. *J. Power Sources* 307, 806–814. doi:10.1016/j.jpowsour.2016.01.033

Chandrasekaran, R. (2014). Quantification of Bottlenecks to Fast Charging of Lithium-Ion-Insertion Cells for Electric Vehicles. *J. Power Sources* 271, 622–632. doi:10.1016/j.jpowsour.2014.07.106

Chen, H., Zheng, M., Qian, S., Ling, H. Y., Wu, Z., Liu, X., et al. (2021). Functional Additives for Solid Polymer Electrolytes in Flexible and High-energy-density Solid-state Lithium-ion Batteries. *Carbon Energy* 3 (6), 929–956. doi:10.1002/cey2.146

Choi, J., and Park, H. (2022). Correlation between Changes in Environmental Temperature and Performance of High-Discharge Lithium-Polymer Batteries [J]. *Front. Energy Res.*, 10. doi:10.3389/fenrg.2022.830581

Doyle, M., and Newman, J. (1995). The Use of Mathematical Modeling in the Design of Lithium/polymer Battery Systems[J]. *Electrochimica Acta* 40 (13-14), 2191–2196. doi:10.1016/0013-4686(95)00162-8

Ecker, M., Shafiei Sabet, P., and Sauer, D. U. (2017). Influence of Operational Condition on Lithium Plating for Commercial Lithium-Ion Batteries - Electrochemical Experiments and Post-mortem-analysis. *Appl. Energy* 206, 934–946. doi:10.1016/j.apenergy.2017.08.034

Ecker, M., Shafiei Sabet, P., and Sauer, D. U. (2017). Influence of Operational Condition on Lithium Plating for Commercial Lithium-Ion Batteries - Electrochemical Experiments and Post-mortem-analysis. *Appl. Energy* 206, 934–946. doi:10.1016/j.apenergy.2017.08.034

Fan, J., and Tan, S. (2006). Studies on Charging Lithium-Ion Cells at Low Temperatures. *J. Electrochem. Soc.* 153 (6), A1081. doi:10.1149/1.2190029

Fleischhammer, M., Waldmann, T., Bisle, G., Hogg, B.-I., and Wohlfahrt-Mehrens, M. (2015). Interaction of Cyclic Ageing at High-Rate and Low Temperatures and Safety in Lithium-Ion Batteries. *J. Power Sources* 274, 432–439. doi:10.1016/j.jpowsour.2014.08.135

Gao, F., and Tang, Z. (2008). Kinetic Behavior of $LiFePO_4$/C Cathode Material for Lithium-Ion Batteries. *Electrochimica Acta* 53 (15), 5071–5075. doi:10.1016/j.electacta.2007.10.069

Gao, X., Liu, X., and Xie, W. (2021). Multiscale Observation of Li Plating for Lithium-Ion Batteries[J]. *Rare Met.* 40 (11), 3038. doi:10.1007/s12598-021-01730-3

Guan, P., Liu, L., and Gao, Y. (2018). Phase-Field Modeling of Solid Electrolyte Interphase (SEI) Cracking in Lithium Batteries. *ECS Trans.* 85 (13), 1041–1051. doi:10.1149/08513.1041ecst

Han, S., Tang, Y., and Khaleghi Rahimian, S. (2021). A Numerically Efficient Method of Solving the Full-Order Pseudo-2-dimensional (P2D) Li-Ion Cell Model. *J. Power Sources* 490, 229571. doi:10.1016/j.jpowsour.2021.229571

Hein, S., and Latz, A. (2016). Influence of Local Lithium Metal Deposition in 3D Microstructures on Local and Global Behavior of Lithium-Ion Batteries. *Electrochimica Acta* 201, 354–365. doi:10.1016/j.electacta.2016.01.220

Jaguemont, J., Boulon, L., and Dubé, Y. (2016). A Comprehensive Review of Lithium-Ion Batteries Used in Hybrid and Electric Vehicles at Cold Temperatures. *Appl. Energy* 164, 99–114. doi:10.1016/j.apenergy.2015.11.034

Jiang, J., Ruan, H., Sun, B., Zhang, W., Gao, W., Wang, L. Y., et al. (2016). A Reduced Low-Temperature Electro-Thermal Coupled Model for Lithium-Ion Batteries. *Appl. Energy* 177, 804–816. doi:10.1016/j.apenergy.2016.05.153

Khalik, Z., Bergveld, H., and Donkers, M. C. F. (2019). "On Trade-Offs between Computational Complexity and Accuracy of Electrochemistry-based Battery Models," in IEEE 58th Conference on Decision and Control (CDC), 7740–7745. doi:10.1109/CDC40024.2019.9029977

Klett, M., Eriksson, R., Groot, J., Svens, P., Ciosek Högström, K., Lindström, R. W., et al. (2014). Non-uniform Aging of Cycled Commercial $LiFePO_4$//graphite Cylindrical Cells Revealed by Post-mortem Analysis. *J. Power Sources* 257, 126–137. doi:10.1016/j.jpowsour.2014.01.105

Koleti, U. R., Rajan, A., Tan, C., Moharana, S., Dinh, T. Q., and Marco, J. (2020). A Study on the Influence of Lithium Plating on Battery Degradation. *Energies* 13 (13), 3458. doi:10.3390/en13133458

Legrand, N., Knosp, B., Desprez, P., Lapicque, F., and Raël, S. (2014). Physical Characterization of the Charging Process of a Li-Ion Battery and Prediction of Li Plating by Electrochemical Modelling. *J. Power Sources* 245, 208–216. doi:10.1016/j.jpowsour.2013.06.130

Lewerenz, M., Warnecke, A., and Sauer, D. U. (2017). Post-mortem Analysis on $LiFePO_4$ |Graphite Cells Describing the Evolution & Composition of Covering Layer on Anode and Their Impact on Cell Performance. *J. Power Sources* 369, 122–132. doi:10.1016/j.jpowsour.2017.10.003

Li, Y., Gao, X., Qin, Y., Du, J., Guo, D., Feng, X., et al. (2021). Drive Circuitry of an Electric Vehicle Enabling Rapid Heating of the Battery Pack at Low Temperatures. *iScience* 24 (1), 101921. doi:10.1016/j.isci.2020.101921

Lin, X., Khosravinia, K., Hu, X., Li, J., and Lu, W. (2021). Lithium Plating Mechanism, Detection, and Mitigation in Lithium-Ion Batteries. *Prog. Energy Combust. Sci.* 87, 100953. doi:10.1016/j.pecs.2021.100953

Matadi, B. P., Geniès, S., Delaille, A., Chabrol, C., de Vito, E., Bardet, M., et al. (2017). Irreversible Capacity Loss of Li-Ion Batteries Cycled at Low Temperature Due to an Untypical Layer Hindering Li Diffusion into Graphite Electrode. *J. Electrochem. Soc.* 164 (12), A2374–A2389. doi:10.1149/2.0491712jes

Momeni Boroujeni, S., and Birke, K. P. (2019). Study of a Li-Ion Cell Kinetics in Five Regions to Predict Li Plating Using a Pseudo Two-Dimensional Model. *Sustainability* 11 (22), 6392. doi:10.3390/su11226392

Müller, D., Dufaux, T., and Birke, K. P. (2019). Model-Based Investigation of Porosity Profiles in Graphite Anodes Regarding Sudden-Death and Second-Life of Lithium Ion Cells[J]. *Batteries* 5 (2), 49. doi:10.3390/batteries5020049

Onat, N., Kucukvar, M., and Tatari, O. (2014). Towards Life Cycle Sustainability Assessment of Alternative Passenger Vehicles. *Sustainability* 6, 9305–9342. doi:10.3390/su6129305

Ouyang, M., Chu, Z., Lu, L., Li, J., Han, X., Feng, X., et al. (2015). Low Temperature Aging Mechanism Identification and Lithium Deposition in a Large Format Lithium Iron Phosphate Battery for Different Charge Profiles. *J. Power Sources* 286, 309–320. doi:10.1016/j.jpowsour.2015.03.178

Plett, G. (2015). *Battery Management Systems. Battery Modeling Volume I[J].*

Reniers, J. M., Mulder, G., and Howey, D. A. (2019). Review and Performance Comparison of Mechanical-Chemical Degradation Models for Lithium-Ion Batteries. *J. Electrochem. Soc.* 166 (14), A3189–A3200. doi:10.1149/2.0281914jes

Ruan, H., Chen, J., Ai, W., and Wu, B. (2022). Generalised Diagnostic Framework for Rapid Battery Degradation Quantification with Deep Learning. *Energy AI*, 100158. doi:10.1016/j.egyai.2022.100158

Schimpe, M., Von Kuepach, M. E., Naumann, M., Hesse, H. C., Smith, K., and Jossen, A. (2018). Comprehensive Modeling of Temperature-dependent Degradation Mechanisms in Lithium Iron Phosphate Batteries. *J. Electrochem. Soc.* 165 (2), A181–A193. doi:10.1149/2.1181714jes

Somerville, L., Bareño, J., Trask, S., Jennings, P., McGordon, A., Lyness, C., et al. (2016). The Effect of Charging Rate on the Graphite Electrode of Commercial Lithium-Ion Cells: A Post-mortem Study. *J. Power Sources* 335, 189–196. doi:10.1016/j.jpowsour.2016.10.002

Stiaszny, B., Ziegler, J. C., Krauß, E. E., Schmidt, J. P., and Ivers-Tiffée, E. (2014). Electrochemical Characterization and Post-mortem Analysis of Aged $LiMn_2O_4$-$Li(Ni_{0.5}Mn_{0.3}Co_{0.2})O_2$/graphite Lithium Ion Batteries. Part I: Cycle Aging. *J. Power Sources* 251, 439–450. doi:10.1016/j.jpowsour.2013.11.080

Sturm, J., Rheinfeld, A., Zilberman, I., Spingler, F. B., Kosch, S., Frie, F., et al. (2019). Modeling and Simulation of Inhomogeneities in a 18650 Nickel-Rich, Silicon-Graphite Lithium-Ion Cell during Fast Charging. *J. Power Sources* 412, 204–223. doi:10.1016/j.jpowsour.2018.11.043

Su, S., Ma, J., Zhao, L., Lin, K., Li, Q., Lv, S., et al. (2021). Progress and Perspective of the Cathode/electrolyte Interface Construction in All-solid-state Lithium Batteries. *Carbon Energy* 3 (6), 866–894. doi:10.1002/cey2.129

Tippmann, S., Walper, D., Balboa, L., Spier, B., and Bessler, W. G. (2014). Low-temperature Charging of Lithium-Ion Cells Part I: Electrochemical Modeling and Experimental Investigation of Degradation Behavior. *J. Power Sources* 252, 305–316. doi:10.1016/j.jpowsour.2013.12.022

Tomaszewska, A., Chu, Z., Feng, X., O'Kane, S., Liu, X., Chen, J., et al. (2019). Lithium-ion Battery Fast Charging: A Review. *eTransportation* 1, 100011. doi:10.1016/j.etran.2019.100011

Waldmann, T., Hogg, B.-I., and Wohlfahrt-Mehrens, M. (2018). Li Plating as Unwanted Side Reaction in Commercial Li-Ion Cells - A Review. *J. Power Sources* 384, 107–124. doi:10.1016/j.jpowsour.2018.02.063

Waldmann, T., Wilka, M., Kasper, M., Fleischhammer, M., and Wohlfahrt-Mehrens, M. (2014). Temperature Dependent Ageing Mechanisms in Lithium-Ion Batteries - A Post-Mortem Study. *J. Power Sources* 262, 129–135. doi:10.1016/j.jpowsour.2014.03.112

Wu, X., Wang, W., and Du, J. (2020). Effect of Charge Rate on Capacity Degradation of $LiFePO_4$ Power Battery at Low Temperature. *Int. J. Energy Res.* 44, 1775–1788. doi:10.1002/er.5022

Xia, L., Najafi, E., Li, Z., Bergveld, H. J., and Donkers, M. C. F. (2017). A Computationally Efficient Implementation of a Full and Reduced-Order Electrochemistry-Based Model for Li-Ion Batteries. *Appl. Energy* 208, 1285–1296. doi:10.1016/j.apenergy.2017.09.025

Xie, W., He, R., Gao, X., Li, X., Wang, H., Liu, X., et al. (2021). Degradation Identification of $LiNi_{0.8}Co_{0.1}Mn_{0.1}O_2$/graphite Lithium-Ion Batteries under Fast Charging Conditions. *Electrochimica Acta* 392, 138979. doi:10.1016/j.electacta.2021.138979

Yang, S., He, R., Zhang, Z., Cao, Y., Gao, X., and Liu, X. (2020). CHAIN: Cyber Hierarchy and Interactional Network Enabling Digital Solution for Battery Full-Lifespan Management. *Matter* 3 (1), 27–41. doi:10.1016/j.matt.2020.04.015

Yang, X.-G., Ge, S., Liu, T., Leng, Y., and Wang, C.-Y. (2018). A Look into the Voltage Plateau Signal for Detection and Quantification of Lithium Plating in Lithium-Ion Cells. *J. Power Sources* 395, 251–261. doi:10.1016/j.jpowsour.2018.05.073

Yang, X.-G., and Wang, C.-Y. (2018). Understanding the Trilemma of Fast Charging, Energy Density and Cycle Life of Lithium-Ion Batteries. *J. Power Sources* 402, 489–498. doi:10.1016/j.jpowsour.2018.09.069

Zhang, G., Wei, X., Han, G., Dai, H., Zhu, J., Wang, X., et al. (2021). Lithium Plating on the Anode for Lithium-Ion Batteries during Long-Term Low Temperature Cycling. *J. Power Sources* 484, 229312. doi:10.1016/j.jpowsour.2020.229312

Zhang, L., Gao, X., Liu, X., Zhang, Z., Cao, R., and Cheng, H. (2022). CHAIN: Unlocking Informatics-Aided Design of Li Metal Anode from Materials to applications[J]. *Rare Metals*, 13. doi:10.1007/s12598-021-01925-8

Zhang, S. S., Xu, K., and Jow, T. R. (2003). The Low Temperature Performance of Li-Ion Batteries. *J. Power Sources* 115 (1), 137–140. doi:10.1016/s0378-7753(02)00618-3

Zhang, S., Xu, K., and Jow, T. (2003). Low-temperature Performance of Li-Ion Cells with a LiBF4-Based Electrolyte. *J. Solid State Electrochem* 7 (3), 147–151. doi:10.1007/s10008-002-0300-9

Zhao, X., Yin, Y., Hu, Y., and Choe, S.-Y. (2019). Electrochemical-thermal Modeling of Lithium Plating/stripping of $Li(Ni_{0.6}Mn_{0.2}Co_{0.2})O_2$/Carbon Lithium-Ion Batteries at Subzero Ambient Temperatures. *J. Power Sources* 418, 61–73. doi:10.1016/j.jpowsour.2019.02.001

Zhao, Y., Choe, S.-Y., and Kee, J. (2018). Modeling of Degradation Effects and its Integration into Electrochemical Reduced Order Model for $Li(MnNiCo)O_2$/Graphite Polymer Battery for Real Time Applications. *Electrochimica Acta* 270, 440–452. doi:10.1016/j.electacta.2018.02.086

Zhou, C.-C., Su, Z., Gao, X.-L., Cao, R., Yang, S.-C., and Liu, X.-H. (2021). Ultra-high-energy Lithium-Ion Batteries Enabled by Aligned Structured Thick Electrode Design. *Rare Metall.* 41 (1), 14–20. doi:10.1007/s12598-021-01785-2

Zhu, J., Dewi Darma, M. S., Knapp, M., Sørensen, D. R., Heere, M., Fang, Q., et al. (2020). Investigation of Lithium-Ion Battery Degradation Mechanisms by Combining Differential Voltage Analysis and Alternating Current Impedance. *J. Power Sources* 448, 227575. doi:10.1016/j.jpowsour.2019.227575

Zhu, J., Knapp, M., Sørensen, D. R., Heere, M., Darma, M. S. D., Müller, M., et al. (2021). Investigation of Capacity Fade for 18650-type Lithium-Ion Batteries Cycled in Different State of Charge (SoC) Ranges. *J. Power Sources* 489, 229422. doi:10.1016/j.jpowsour.2020.229422

Zinth, V., von Lüders, C., Hofmann, M., Hattendorff, J., Buchberger, I., Erhard, S., et al. (2014). Lithium Plating in Lithium-Ion Batteries at Sub-ambient Temperatures Investigated by *In Situ* Neutron Diffraction. *J. Power Sources* 271, 152–159. doi:10.1016/j.jpowsour.2014.07.168

**Conflict of Interest:** The authors declare that the research was conducted in the absence of any commercial or financial relationships that could be construed as a potential conflict of interest.

**Publisher's Note:** All claims expressed in this article are solely those of the authors and do not necessarily represent those of their affiliated organizations, or those of the publisher, the editors and the reviewers. Any product that may be evaluated in this article, or claim that may be made by its manufacturer, is not guaranteed or endorsed by the publisher.